



**HAL**  
open science

# Frottement et lubrification en mise en forme = Numerical modelling of lubricated foil rolling

Michael P.F. Sutcliffe, Pierre Montmitonnet

► **To cite this version:**

Michael P.F. Sutcliffe, Pierre Montmitonnet. Frottement et lubrification en mise en forme = Numerical modelling of lubricated foil rolling. Revue de Métallurgie, 2001, 5, pp.Pages 435-442. 10.1051/metal:2001197 . hal-00574224

**HAL Id: hal-00574224**

**<https://minesparis-psl.hal.science/hal-00574224>**

Submitted on 7 Mar 2011

**HAL** is a multi-disciplinary open access archive for the deposit and dissemination of scientific research documents, whether they are published or not. The documents may come from teaching and research institutions in France or abroad, or from public or private research centers.

L'archive ouverte pluridisciplinaire **HAL**, est destinée au dépôt et à la diffusion de documents scientifiques de niveau recherche, publiés ou non, émanant des établissements d'enseignement et de recherche français ou étrangers, des laboratoires publics ou privés.

# Numerical modelling of lubricated foil rolling

M.P.F. Sutcliffe\*, P. Montmitonnet\*\*

\* Department of Engineering,  
University of Cambridge, Grande-Bretagne

\*\* CEMEF, École des Mines de Paris, Sophia Antipolis

**A model of lubricated cold strip rolling (1, 2) is extended to the thin foil regime. The model considers the evolution of asperity geometry and lubricant pressure through the bite, treating the strip using a conventional slab model. The elastic deflections of the rolls are coupled into the problem using an elastic finite element model. Friction between the roll and the asperities on the strip is modelled using the Coulomb and Tresca friction factor approaches. The shear stress in the Coulomb friction model is limited to the shear yield stress of the strip. A novel modification to these standard friction laws is used to mimic slipping friction in the reduction regions and sticking friction in a central neutral zone. The model is able to reproduce the sticking and slipping zones predicted by Fleck et al. (3). The variation of rolling load, lubricant film thickness and asperity contact area with rolling speed is examined, for conditions typical of rolling aluminium foil from a thickness of 50 to 25  $\mu\text{m}$ . The contact area and hence friction rises as the speed drops, leading to a large increase in rolling load. This increase is considerably more marked using Coulomb friction as compared with the friction factor approach. Forward slip increases markedly as the speed falls and a significant sticking region develops.**

## ■ INTRODUCTION

Industry is increasingly concerned to develop models of cold rolling, both to improve their on-line control, and to optimize mill set-up and scheduling. Two factors make foil modelling particularly demanding. Firstly, it is essential to model the elastic deformation of the rolls accurately. Secondly, as the ratio of the bite length to the strip thickness increases, the load and reduction in gauge become increasingly sensitive to friction, requiring an accurate mathematical model of friction.

The foil rolling model of Fleck et al (3), which has become widely accepted in industry, combines elastic deformation of the rolls and an elastic-plastic model of the foil. They assume that friction between the roll and strip can be modelled using a Coulomb friction coefficient, typically using a value of 0.03. The contact length is split into a series of zones, depending on whether the strip is plastic or elastic and whether there is slip between the roll and strip. At the thinner gauges the solution predicts a central flat, no-slip region, where friction falls below the limiting value for slipping. This model has been extended by Dixon and Yuen (4) and Domanti et al (5). An alternative strategy which overcomes numerical difficulties associated with the above procedure is described by Gratacos et al (6). They define an arbitrary friction law which simulates sticking friction in the neutral zone and slipping friction elsewhere. Le and Sutcliffe (7) extend this approach using a physically-based friction law in the neutral zone.

An approximation to the lubrication conditions in the contact can be made by estimating the oil film thickness  $h_s$  according to Wilson and Walowit's (8) formula for smooth rolls and strips :

$$h_s = \frac{6\eta_0\alpha\bar{u}}{\theta_0(1 - \exp(-\alpha Y))} \quad [1]$$

where  $\bar{u} = (u_r + u_{s0})/2$  is the mean of the roll and strip inlet speeds,  $\theta_0$  is the inlet angle between the strip and roll and  $Y$  is the plain strain yield strength of the strip.  $\eta_0$  is the viscosity of the lubricant at ambient pressure and  $\alpha$  is the Barus pressure viscosity coefficient. The ratio  $\Lambda_s = h_s/\sigma_{r0}$  of the smooth film thickness  $h_s$  to the combined roll and initial strip roughness  $\sigma_{r0}$  is used to characterize the lubrication regime. In industrial rolling, the needs for high productivity but good surface finish dictate that rolling is commonly in the "mixed" regime with  $\Lambda_s$  between 0.01 and 0.5.

Manuscrit reçu le 20 juin 2000, bon à publier le 5 octobre 2000.

© La Revue de Métallurgie 2001.

## Un modèle de lubrification en laminage à froid

M.P.F. Sutcliffe\*, P. Montmitonnet\*\*

\* Department of Engineering,  
University of Cambridge, Grande-Bretagne

\*\* CEMEF, École des Mines de Paris, Sophia Antipolis

*Le laminage des métaux en feuille mince met en œuvre un fort couplage entre la déformation des cylindres et celle de la feuille, qui se traduit par de sérieuses difficultés de convergence des modèles d'une part, et une mécanique particulière : très grande sensibilité au frottement (donc à la lubrification), contact des cylindres de part et d'autre de la feuille (« roll kiss »), apparition d'une zone très déformée, quasi-plate, sur la surface de contact avec le cylindre, où le métal, en déformation élastique, a la vitesse du cylindre (« zone collante » ou « zone neutre »).*

*Le modèle de lubrification en régime mixte du laminage à froid de tôle (1, 2) présenté dans ce numéro (Montmitonnet et al.) a donc été adapté à ce laminage en très faible épaisseur. Il prend en compte l'évolution de la géométrie des aspérités et de la pression du lubrifiant le long de l'emprise [7], la tôle étant traitée par un modèle de tranches classique [5], [6]. On y couple la déformation élastique des cylindres, dont le calcul fait appel à la méthode des éléments finis. Le frottement entre le cylindre et la rugosité de la tôle est représenté au choix par les modèles de Coulomb ou de Tresca [2]. Dans le premier cas, la contrainte de cisaillement est limitée par la contrainte d'écoulement en cisaillement de la tôle. On introduit une nouvelle modification à ces lois standard (équ. [3], fig. 1) pour simuler le frottement glissant dans les zones de réduction et le frottement collant dans la zone neutre centrale. Le modèle est ainsi capable de reproduire la co-existence de zones glissantes et collantes (fig. 2 et 4) prédites par Fleck et al. (3).*

*On examine les variations de force de laminage, d'épaisseur de film lubrifiant et d'aire réelle de contact avec la vitesse de laminage, pour des conditions typiques du laminage d'aluminium en feuille mince, de 50 à 25  $\mu\text{m}$ . L'aire réelle de contact, donc le frottement, croît lorsque la vitesse diminue, du fait du moindre entraînement d'huile par effet hydrodynamique. Cela provoque une augmentation de la force de laminage (jusqu'à un facteur 40 entre 40  $\text{m}\cdot\text{s}^{-1}$  et 10  $\text{m}\cdot\text{s}^{-1}$  !), considérablement plus marquée si on utilise un frottement de Coulomb plutôt que celui de Tresca. Le glissement en avant augmente notablement quand la vitesse diminue, atteignant les très hautes valeurs rencontrées en pratique (jusqu'à 45 %, pour une réduction d'épaisseur de 50 %). La réduction s'effectue exclusivement en entrée et sortie de l'emprise (voir fig. 3), l'épaisseur de la feuille restant constante dans la partie centrale, où le contact est d'ailleurs collant (vitesse relative nulle).*

*On compare la loi de Coulomb et la loi de Tresca, les valeurs des coefficients ( $\mu_a = 0,1$ ,  $m_a = 0,25$ ) étant choisies pour donner la même force de laminage à grande vitesse. La loi de Tresca se caractérise par l'absence d'effet « boule-de-neige » que subit la loi de Coulomb (lorsque la vitesse diminue, le frottement augmente ; la pression de contact croît rapidement, ce qui augmente les contraintes de frottement, et ainsi de suite). Les variations de la force ou du glissement en avant avec la vitesse sont donc ralenties.*

Various tribological models have been described recently for cold strip rolling (2, 9-12). The change in oil pressure is modelled using Reynolds equation, suitably modified to include the effect of roughness. The effect of bulk deformation on the asperity crushing behaviour can be described using the results of Sutcliffe (13) or Wilson and Sheu (14). Two approaches have been used to combine the lubrication details with an overall model of the bite. Either an inlet analysis can be used, in which it is assumed that the tribology of the contact is determined in a short inlet region (11). Alternatively, the plasticity and tribological details are modelled through the bite (9, 10, 12). These models calculate the variation of lubricant film thickness through the bite and hence the area of contact ratio  $A$ , i.e. the fraction of the surface for which the asperity tops are in contact. The remain-

ing valley regions are separated by oil. The friction stress is found by adding contributions from these two areas. Results show that the film thickness and area of contact ratio depend primarily on the rolling speed, oil properties and inlet geometry. The effects of yield stress, strip thickness, asperity geometry and unwind tension are of secondary importance. Experimental measurements of film thickness are in good agreement with theoretical predictions (10, 15).

For foil rolling, it is necessary to model both roll elastic deformation and the tribology. Marsault et al. (1, 2) describe such a model, but only consider the case where there is limited roll elasticity. In this paper that model is extended to the thin foil regime where there is a central flat section.

**NOTATIONS**

- $A$  : area of contact ratio
- $h_t$  : mean film thickness, averaged across the width of the contact
- $h_s$  : smooth film thickness, using the Wilson and Walowit formula, equation [1]
- $k$  : shear yield stress of the strip ( $k = Y/\sqrt{3}$  for the von Mises yield criterion).
- $m_a, m_b$  : friction factor for the areas of contact and valleys
- $p$  : mean contact pressure between roll and strip
- $p_a, p_b$  : pressure on the asperity tops and in the valleys
- $R$  : roll radius
- $t, t_0$  : strip thickness, inlet thickness
- $\bar{u}$  : mean entraining velocity,  $\bar{u} = (u_r + u_s)/2$
- $u_r, u_s (u_s0)$  : roll and strip speed (at the inlet)
- $x$  : co-ordinate in rolling direction
- $Y$  : plane strain yield stress of the strip
- $\alpha$  : oil pressure viscosity index
- $\delta$  : Knock-down factor for frictional stress in the sticking region
- $\varepsilon$  : tolerance for strip slope in sticking region
- $\eta (\eta_0)$  : viscosity of lubricant (at ambient pressure)
- $\lambda$  : wavelength of the surface roughness
- $\Lambda_s$  : speed parameter,  $\Lambda_s = h_s/\sigma_{r0}$
- $\mu_a, \mu_b$  : Coulomb friction coefficient for the areas of contact and valleys
- $\theta, \theta_0, \theta_1$  : roll slope, at the inlet and at a representative point in the bite (see fig. 3)
- $\sigma_r (\sigma_{r0})$  : combined r.m.s. surface roughness of the strip and roll (initial roughness)
- $\sigma_x$  : longitudinal tension stress
- $\tau$  : mean shear stress between roll and strip
- $\tau_a, \tau_b$  : shear stress for the areas of contact and valleys

where  $p_a$  is the pressure on the asperity tops and  $k$  is the shear yield stress of the workpiece. With the Coulomb friction model, it is necessary to include the additional limitation that the friction stress cannot exceed the shear yield stress of the strip. With the slab model used to model the strip, frictional shear stresses are not included when considering the yield condition for the strip, so that this limit is not otherwise imposed.

To simulate the sticking region, where the shear stress falls below the value for slipping friction (equation [2]), the approach of Gratacos et al (6) is followed in adopting an arbitrary friction law. A knockdown factor  $\delta$  on the limiting friction is applied to [2], so that  $\tau_a = \delta\mu_a p_a$  or  $\delta m_a k$ , with :

$$\delta = \frac{\theta}{\sqrt{\theta^2 + (\varepsilon\theta_1)^2}} \quad [3]$$

where  $\varepsilon$  is a tolerance parameter,  $\theta$  the local roll slope and  $\theta_1$  a representative roll slope in a slipping region (see fig. 3). Here  $\theta_1$  is taken as the slope at the middle of the first reduction region. This variation of  $\delta$  with  $\theta/\theta_1$  is sketched in figure 1. For  $\theta/\theta_1 \ll \varepsilon$  the frictional stress is approximately proportional to the roll slope while, for  $\theta/\theta_1 \gg \varepsilon$ ,  $\delta$  approaches one and friction takes its limiting value of  $\mu_a p_a$  or  $m_a k$ . Changes in friction in the central sticking region can be accommodated by small deviations in flatness. As long as  $\varepsilon$  is sufficiently small, the roll stays essentially flat there and the solution is unaffected by the exact form of the friction law. Typically a value of  $\varepsilon = 0.1$  was found appropriate. A physically-based argument for a friction law of this form is presented by Le and Sutcliffe (7).

The shear stress in the valleys  $\tau_b$  is estimated from the Newtonian viscous behaviour of the oil, with a constant valley depth of  $h_t/(1-A)$ , where  $h_t$  is the mean film thickness. The lesser of this hydrodynamic estimate and the corresponding shear stress  $\tau_a$  on the asperity tops is used for the valley regions. The average shear stress  $\tau$  is given by a weighted sum of the asperity and valley contributions :

$$\tau = A\tau_a + (1-A)\tau_b \quad [4]$$

■ **THEORY**

Most of the modelling and numerical implementation is taken directly from the work of Marsault (1) and only an outline is given here. To extend the model into the thin foil regime where the roll deformations are large, a new friction model is introduced, as described below, to overcome numerical difficulties with Marsault's formulation.

**Friction modelling**

Fleck et al (3) show that both slipping and sticking between the roll and strip need to be considered in foil rolling. For the regions of slipping, either a Coulomb friction coefficient  $\mu_a$  or a Tresca friction factor  $m_a$  is used to estimate the shear stress  $\tau_a$  on the asperity tops as :

$$\tau_a = \mu_a p_a \text{ or } \tau_a = m_a k \quad [2]$$

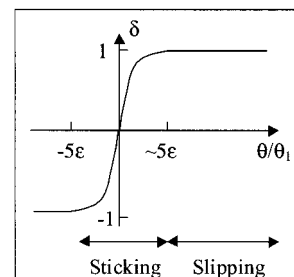


Figure 1 – Schematic variation in knockdown factor  $\delta$  with roll slope  $\theta$  used to simulate sticking and slipping friction.

Figure 1 – Schéma des variations du facteur d'atténuation  $\delta$  en fonction de la pente  $\theta$  de la surface du cylindre, tel qu'utilisé pour simuler le frottement glissant et le frottement collant.

### Strip deformation

A standard slab model is used for the strip. Equilibrium for a slab in the bite gives :

$$t \frac{d\sigma_x}{dx} + (\sigma_x + p) \frac{dt}{dx} + 2\tau = 0 \quad [5]$$

where  $x$  is the distance in the rolling direction,  $t$  the strip thickness,  $\sigma_x$  the tensile stress in the rolling direction and  $p$  the average contact pressure. In the inlet and exit regions, where there is no plastic deformation, it is assumed that the strip is linear-elastic. In the central reduction region, the strip is taken as perfectly plastic, and at the point of yield, so that :

$$\sigma_x + p = Y \quad [6]$$

In principle there can be elastic unloading in the flat central region of the bite. However, as long as the roll remains essentially flat in this region, this detail can be neglected. In these circumstances, the pressure distribution is effectively independent of the constitutive model in this region, instead being determined by the pressure needed to generate a flat on the roll.

### Roll elasticity

A standard elastic FEM package is used to solve the roll deformation equations for a given pressure distribution. The roll surface deformations relative to the centre of the roll are calculated and the approach of centres of the rolls updated between iterations to maintain a constant strip reduction. Cubic splines are used to interpolate between node points in the FE model for integrating the hydrodynamic equations.

### Hydrodynamic modelling

The variation in oil pressure  $p_b$  through the bite is given by Reynolds equation, modified to include the effect of roughness :

$$\phi_x \frac{h_t}{12\eta} \frac{dp_b}{dx} = \frac{u_x + u_r}{2} h_t + \frac{u_x - u_r}{2} \sigma_t \phi_s - Q \quad [7]$$

where  $u_x$  is the local strip velocity and  $Q$  a flow rate constant. Flow factors  $\phi_x$  and  $\phi_s$ , which are functions of the mean film thickness  $h_t$  and the combined strip and roll roughness  $\sigma_p$ , are derived by Wilson and Marsault (16), using the results of Patir and Cheng (17) and Lo (18). They also depend on  $\gamma$ , the ratio of roughness correlation lengths in the rolling and transverse direction. Here  $\gamma$  is taken equal to 9, appropriate for nearly longitudinal roughness. To avoid numerical instabilities, the Poiseuille term is dropped in the work zone where appropriate. As the oil film becomes smaller, Lo shows that a 'percolation threshold' is eventually reached when individual pockets of oil become trapped. This occurs, for longitudinal roughness with  $\gamma = 9$ , when  $h_t/\sigma_t = 0,038$ . For the results presented here, the film thicknesses are significantly greater than this percolation threshold. Where the film thickness approaches the percolation threshold, micro-plasto-hydrodynamic models are needed (19).

### Asperity Flattening

To derive an accurate estimate of the change in asperity geometry and contact area through the bite, it is essential to include the effect of bulk plasticity on changes in asperity deformation. Here Sutcliffe's (20) model for crushing of longitudinal roughness is used. This uses a curve fit to the finite element calculations of Korzekwa (21), and is qualitatively similar to the asperity crushing model of Sheu and Wilson (14).

### Numerical method

The details of the numerical method are described in detail by Marsault et al. (1, 2). A double-shooting procedure is used to find the inlet strip speed and oil flow rate constant  $Q$  for a given roll shape. The differential equations for the variation of pressure and contact ratio through the bite are integrated using a Runge-Kutta method. As the integration proceeds, the appropriate equations are changed, according to the local conditions (e.g. elastic or plastic strip, inclusion of the Poiseuille term in the Reynolds equation). Once a converged pressure distribution is found, the corresponding strip shape  $t_C$  is solved using the FE model for the roll elastic deformations. The roll shape is updated using a relaxation method, until the change in roll shape is within a suitably small tolerance. The new roll shape  $t_{N+1}$  is related to the old roll shape  $t_N$  and the computed roll shape  $t_C$ , based on the current pressure distribution, by the relaxation formula :

$$t_{N+1} = \beta t_C + (1 - \beta) t_N \quad [8]$$

Typically a relaxation coefficient  $\beta$  between 0.2 and 0.05 is suitable, giving computation times of the order of 2 h on a small super-computer for the most demanding cases.

## ■ RESULTS

In this section we present results typical of industrial rolling of aluminium foil from a thickness of 50 to 25  $\mu\text{m}$ , lubricated with a standard rolling oil. For these conditions there is significant roll elasticity. Coiling tensions are applied on the unwind and rewind sides. Conditions are detailed in *table 1*.

*Figure 2* shows the distribution of average pressure  $p$ , average shear stress  $\tau$  and area of contact ratio  $A$  for a rolling speed of 20 m/s with a Coulomb friction factor  $\mu_a = 0.1$ . The normal pressure is normalized by the yield stress  $Y$  and the shear stress by  $\mu_a Y$ , so that the shear curve lies on the pressure curve when the effective contact area  $A$  and the friction knockdown factor  $\delta$  are both equal to one. *Figure 3* shows the corresponding change in strip thickness  $t$  through the bite, normalised by the inlet strip thickness  $t_0$ . These results have a similar form to those of Fleck et al. (3), with a significant « flat » sticking region at the centre of the bite where the shear stress fall below its limiting value. Because of the friction law used, there are in fact small deviations in thickness in this central region, but these are so slight as to be

TABLE I – Summary of conditions.

TABLEAU I – Résumé des conditions de laminage.

Strip	Entry gauge	50 $\mu\text{m}$
	Exit gauge	25 $\mu\text{m}$
	Yield stress	150 MPa
	Unwind tension	20 MPa
	Rewind tension	20 MPa
	Young's modulus	70 Gpa
	Poisson's ratio	0.3
	Rolls	Radius
Roll peripheral speed		5 - 40 m/s
Young's modulus		210 GPa
Poisson's ratio		0.3
Surfaces	Combined r.m.s. amplitude	0.3 $\mu\text{m}$
	Asperity wavelength	30 $\mu\text{m}$
	Asperity friction	$\mu_a = 0.1$ or $m_a = 0.25$
Lubricant	Viscosity at ambient pressure	$2.5 \times 10^{-3}$ Pas
	Pressure viscosity coefficient	$1.2 \times 10^{-8}$ m <sup>2</sup> /N

scarcely visible in *figure 3*. The relaxation technique used to update the roll shape has converged automatically on the shape in the central flat region which gives the appropriate sticking friction distribution compatible with the elastic deformations of the roll. *Figure 2* shows that, for the Coulomb friction model, the frictional stress equals the shear yield stress of the strip over a significant portion of the exit reduction region (where the shear stress has a plateau). Because of the high pressures directly after this region of the bite, the estimated hydrodynamic shear stress would exceed the asperity shear stress. Hence the average shear stress is taken equal to  $\mu_a p$ , the effective contact area equals one and the curves for shear and normal pressure lie on top of one another.

Details at the inlet are illustrated in *figure 4*, showing the change in normal pressure  $p$ , asperity and hydrodynamic pressures  $p_a$  and  $p_b$  and area of contact ratio  $A$ . Comparing the scales on *figures 2 and 4* it is clear that the inlet region is very short compared with the length of the bite. At the beginning of the inlet, before the hydrodynamic pressure has built up, the asperity pressure is approximately equal to the hardness  $3Y$ . As the pressure in the lubricant build ups, the strip yields, causing a sharp change in the slope of the mean pressure curve and a drop in the asperity pressure. At this point, the asperity tops are rapidly flattened and the valley pressure rapidly rises to equal the asperity pressure.

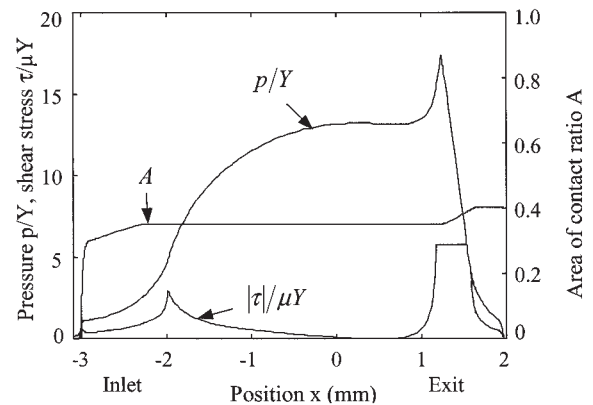


Figure 2 – Variation in pressure, shear stress and area of contact ratio through the bite ;  $u_r = 20$  m/s,  $\mu_a = 0.1$ .

Figure 2 – Variation le long de l'emprise de la pression de contact, de la contrainte de cisaillement et de l'aire réelle de contact ;  $u_r = 20$  m/s,  $\mu_a = 0,1$ .

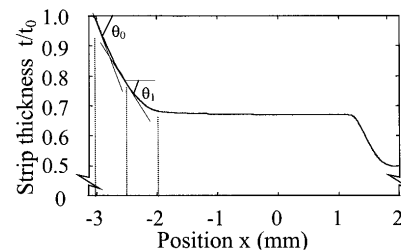


Figure 3 – Variation in strip thickness through the bite,  $u_r = 20$  m/s,  $\mu_a = 0.1$ . Angle  $\theta$  is the local slope of the roll profile,  $\theta_0$  its value at bite entry,  $\theta_1$  at the centre of the first deformation zone.

Figure 3 – Variation le long de l'emprise de l'épaisseur de la tôle.  $u_r = 20$  m/s,  $\mu_a = 0,1$ . L'angle  $\theta$  est la pente locale au profil du cylindre,  $\theta_0$  sa valeur au point d'entrée,  $\theta_1$  au centre de la première zone de déformation.

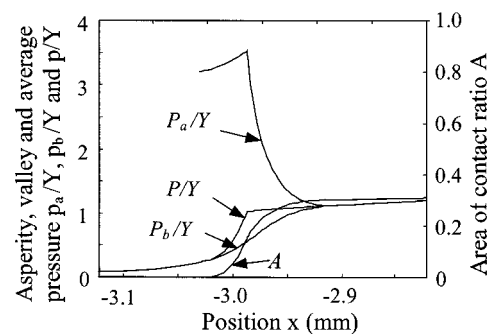


Figure 4 – Variation of asperity, valley and average pressure and area of contact ratio in the inlet ;  $u_r = 20$  m/s,  $\mu_a = 0.1$ .

Figure 4 – Zone d'entrée : variation des pressions sur les aspérités, dans les vallées et moyenne, ainsi que de l'aire réelle de contact ;  $u_r = 20$  m/s,  $\mu_a = 0,1$ .

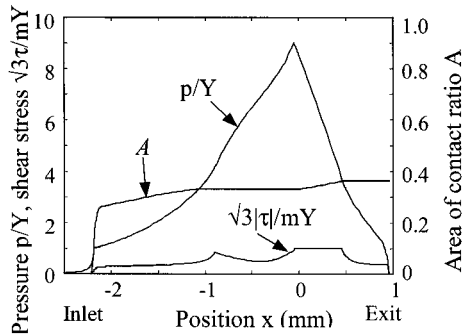


Figure 5 – Variation in pressure, shear stress, and area of contact ratio through the bite ;  $u_r = 20$  m/s,  $m_a = 0.25$ .

Figure 5 – Variation le long de l'emprise de la pression de contact, de la contrainte de cisaillement et de l'aire réelle de contact ;  $u_r = 20$  m/s,  $m_a = 0.25$ .

Through the remainder of the bite, the model assumes that the valley pressure  $p_b$  remains equal to the asperity pressure  $p_a$ . The area of contact ratio  $A$  increases slightly through the rest of the bite due to thinning of the oil film as the strip surface elongates, fig. 2.

Figure 5 shows the variation through the bite of the normal pressure  $p$ , the shear stress  $\tau$  and area of contact ratio  $A$ , for the same conditions as figure 2, but with a friction factor  $m_a = 0.25$  instead of a friction coefficient  $\mu_a = 0.1$ . These values of friction factor and friction coefficient have been chosen for comparison to give approximately the same mean frictional stress and rolling loads at high rolling speeds where there is only a slight friction hill. (In fact the two laws give the same stress for  $p = 1.4Y$ .) The friction factor approach gives lower shear stresses in the high pressure regions where  $p > 1.4Y$ , and so a significantly lower average pressure. The frictional stresses are normalised by  $m_a Y / \sqrt{3}$ , so that this expression equals one when the effective contact area and the friction knockdown factor  $\delta$  are both equal to one.

Effect of speed

Figure 6 shows the effect of rolling speed on roll load, using a logarithmic axis for load. The change in speed from 5 to 40 m/s corresponds to a range of film thickness parameter  $\Lambda_s$  from 0.22 to 1.76<sup>(\*)</sup>. The graph includes the cases of a friction coefficient of 0.1 and a Tresca friction factor of 0.25. Corresponding changes in the forward slip and the mean film thickness  $h_f / \sigma_{t0}$  and area of contact ratio  $A$  at the exit are plotted in figure 7. As the speed falls, there is a reduction in the thickness of the oil film drawn through the contact  $h_f / \sigma_{t0}$  and the area of contact ratio rises accordingly. The associated increase in frictional stress causes a large increase in rolling load, as observed experimentally. A flat region in the bite is predicted below speeds of about 20 and 30 m/s for

\* Although the smooth film thickness, equation [1], is based on the slope of the undeformed roll at the inlet, in fact the slope of the deformed roll is not very different for the cases presented here. Hence this smooth film thickness is representative.

the friction coefficient and friction factor approaches, respectively. The marked difference in load between the Tresca and Coulomb friction models, fig. 6, reflects the sensitivity of results to the details of the friction distribution, despite the relatively slight changes in the film thickness and area of contact estimates (fig. 7).

Forward slip is a useful indicator of the strip shape in the bite, as well as being an important variable for control purposes. Figure 7 shows that an increase in forward slip from about 5 to 45 % is predicted with the Coulomb model as the speed falls and a flat central region develops. The increase in forward slip is much less marked for the Tresca friction model. There are larger frictional tractions at the exit than at the entry, both on account of the increase in area of contact ratio through the bite and due to the larger hydrodynamic friction component at the higher pressures in the exit half of the bite. This tends to inhibit strip reduction at the exit leading to smaller values of forward slip than predicted by the constant friction coefficient model of Fleck et al (3).

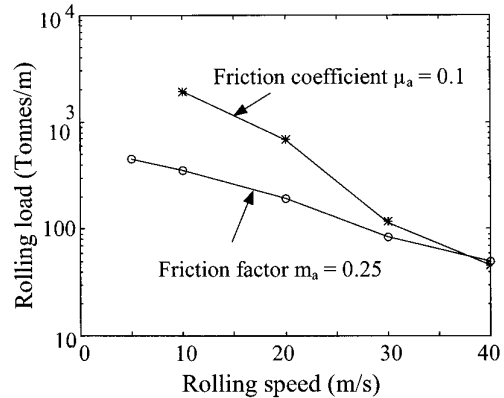


Figure 6 – Effect of rolling speed on roll load.

Figure 6 – Effet de la vitesse sur la force de laminage.

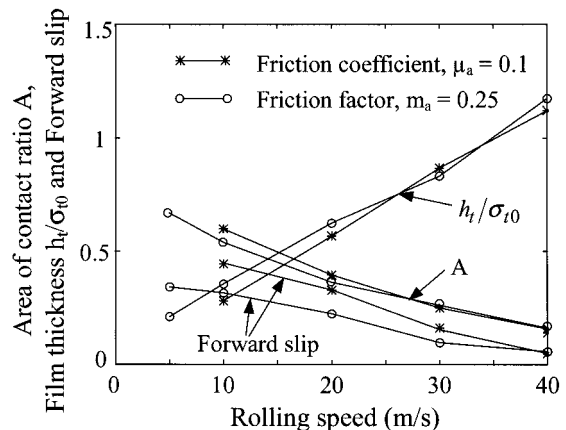


Figure 7 – Effect of rolling speed on area of contact ratio, film thickness and forward slip.

Figure 7 – Effet de la vitesse sur l'aire réelle de contact, l'épaisseur de film et le glissement en avant.

## ■ DISCUSSION

Figures 6 and 7 confirm that the key rolling parameters – load and forward slip – are sensitive to the details of the frictional model. An appropriate choice of friction model must rely either on a comparison with experimental measurements or some physical insight into the interface behaviour in the bite. Both approaches are currently being explored. As figure 4 shows, the inlet region is very short compared with the bite region for the conditions considered here. Sutcliffe and Johnson (11) explained why this could be expected with mixed lubrication and typical roll roughnesses and strip reductions, while Le and Sutcliffe (22) have constructed a regime map for thick strip rolling which shows that this is true for most practical purposes. With foil rolling, the small value of  $t/\lambda$ , the ratio of the strip thickness to the roughness wavelength, increases the ease with which asperities can be crushed. Hence the inlet will be small compared with the bite over an even wider range of operating conditions. This observation suggests that it would be appropriate in most cases to consider all the tribological details only in the inlet. A much-simplified model of the contact could be used to estimate the change in friction through the bite. With this approach there is limited coupling between roll deformation and lubrication, which would give a much simpler and more robust analysis.

The characteristic roughness wavelength  $\lambda$  was taken in this analysis as 30  $\mu\text{m}$ . Sutcliffe and Le (20, 22) investigate the effect of roughness wavelength, considering more than one wavelength. Their results and subsequent work in progress suggest this single value characterizes the spectrum of roughness reasonably well for typical aluminium foil rolling conditions.

## ■ CONCLUSIONS

A tribological model of cold strip rolling (1, 2) is extended to the thin foil rolling where the elastic deflections of the rolls become significant. This model calculates the variation of asperity geometry and lubricant pressure through the bite and uses a conventional slab model of the strip. An elastic finite element model is used to calculate roll deflections. A previous model of foil rolling (3) predicts reduction zones at the entry and exit to the bite, with a flat neutral zone where there is limited relative slip between the roll and strip. This observation is used to construct an arbitrary modification to the standard friction laws which simulates this behaviour, with friction proportional to the roll slope in the sticking region and equal to the limiting friction value in the slipping regions. Either Coulomb and Tresca friction models are used in the slipping regions for contact between the rolls and asperity tops, while the frictional stress in the valleys is estimated from the viscous shearing of the oil. In the case of Coulomb friction, the frictional stress is limited to the shear yield stress of the strip.

Results are calculated for typical industrial conditions, rolling aluminium foil from a thickness of 50 to 25  $\mu\text{m}$ . In a short inlet region, the pressure rises in the lubricant until bulk yield-

ing takes place. At that point the asperities are rapidly crushed until the lubricant and asperity pressures equalize. Through the rest of the bite there is a more modest increase in area of contact ratio associated with thinning of the oil film as the strip elongates. Predictions of rolling load using Coulomb friction are significantly higher than those using a friction factor approach. A correct choice of friction model will depend on experimental observations or further physical insight into the behaviour in the bite. The effect of a variation in rolling speed from 5 to 40 m/s on rolling load, film thickness and contact area is examined. As the speed falls, there is a decrease in the amount of oil drawn into the bite and so an increase in area of contact ratio. The associated increase in friction causes a significant increase in rolling load. This is in line with experimental observations. As the speed falls, the forward slip is predicted to increase from a value of 5 to 45 % for the Coulomb friction model. The increase in forward slip is much less marked for the Tresca friction model. Finally, it is suggested that in many circumstances it would be appropriate to simplify the model by calculating the details of the tribology only in the short inlet region. This would improve convergence and robustness considerably.

## Acknowledgements

The authors are most grateful for the advice provided by Drs. Gratacos and Marsault and for the financial help and equipment provided by the CEMEF group at the École des Mines de Paris.

## references

- (1) MARSAULT (N.) – Modélisation du régime de lubrification mixte en laminage à froid. PhD Thesis, École Nationale Supérieure des Mines de Paris (1998).
- (2) MARSAULT (N.), MONTMITONNET (P.), DENEUVILLE (P.), GRATACOS (P.) – A model of mixed lubrication for cold rolling of strip. Proc. NUMIFORM 98, Twente University, Netherlands, A.A. Balkema (Rotterdam) (1998), p. 715-720.
- (3) FLECK (N.A.), JOHNSON (K.L.), MEAR (M.E.), ZHANG (L.C.) – Cold rolling of foil. *Proc. Instn. Mech. Engrs*, 206 (1992), p. 119-131.
- (4) DIXON (A.E.), YUEN (W.Y.D.) – A computationally fast method to model thin strip rolling. Proc. Computational Techniques and Application Conference (1995), p. 239-246.
- (5) DOMANTI (S.A.), EDWARDS (W.J.), THOMAS (P.J.), CHEFNEUX (L.) – Application of foil rolling models to thin steel strip and temper rolling. Proc. 6th International Rolling Conference, Düsseldorf (1994), p. 422-429.
- (6) GRATACOS (P.), MONTMITONNET (P.), FROMHOLZ (C.), CHENOT (J.L.) – A plane-strain elastic finite-element model for cold rolling of thin strip. *Int. J. Mech. Sci.*, 34, 3 (1992), p. 195-210.
- (7) LE (H.R.), SUTCLIFFE (M.P.F.) – A robust model for rolling of thin strip and foil. *Int. J. Mech. Sci.*, 43 (1999), 1405-1419.
- (8) WILSON (W.R.D.), WALOWIT (J.A.) – An isothermal hydrodynamic lubrication theory for strip rolling with front and back tension. Proc. 1971 Tribology Convention, I. Mech. E., London (1972), p. 164-172.

- (9) LIN (H.S.), MARSAULT (N.), WILSON (W.R.D.) – A mixed lubrication model for cold strip rolling. Part I. **Theoretical Tribology Trans.**, 41 (1998), p. 317-326.
- (10) SHEU (S.), WILSON (W.R.D.) – Mixed lubrication of strip rolling. **STLE Trib. Trans.**, 37 (1994), p. 483-493.
- (11) SUTCLIFFE (M.P.F.), JOHNSON (K.L.) – Lubrication in cold strip rolling in the “mixed” regime. **Proc. Instn. Mech. Engrs.**, 204 (1990), p. 249-261.
- (12) CHANG (D.F.), WILSON (W.R.D.), MARSAULT (N.) – Lubrication of strip rolling in the low-speed mixed regime. **Trib. Trans.**, 39 (1996), p. 407-415.
- (13) SUTCLIFFE (M.P.F.) – Surface asperity deformation in metal forming processes. **Int. J. of Mech. Sci.**, 30 (1988), p. 847-868.
- (14) WILSON (W.R.D.), SHEU (S.) – Real area of contact and boundary friction in metal forming. **Int. J. Mech. Sci.**, 30 (1988), p. 475-489.
- (15) SUTCLIFFE (M.P.F.), JOHNSON (K.L.) – Experimental measurements of lubricant film thickness in cold strip rolling. **Proc. Instn Mech. Engrs.**, 204 (1990), p. 263-273.
- (16) WILSON (W.R.D.), MARSAULT (N.) – Partial hydrodynamic lubrication with large fractional contact areas. **ASME J. Tribology**, 120 (1998), p. 1-5.
- (17) PATIR (N.), CHENG (H.S.) – An average flow model for determining effects of three dimensional roughness on partial hydrodynamic lubrication. **ASME J. Lubrication Technology**, 100 (1978), p. 12-17.
- (18) LO (S.W.) – A study on the flow phenomena in the mixed lubrication regime by porous medium model. **ASME J. Tribology**, 116 (1994), p. 640-647.
- (19) LO (S.W.), WILSON (W.R.D.) – A theoretical model of micro-pool lubrication in metal forming. **ASME J. of Tribology**, 121 (1999), p. 731-738.
- (20) SUTCLIFFE (M.P.F.) – Flattening of random rough surfaces in metal forming processes. **ASME J. Tribology**, 121 (1999), p. 433-440.
- (21) KORZEKWA (D.A.) – Surface asperity deformation during sheet forming. **Int. J. Mech. Sci.**, 34, 7 (1992), p. 521-539.
- (22) SUTCLIFFE (M.P.F.), LE (H.R.) – Measurements of surface roughness in cold metal rolling in mixed lubrication regime. **STLE Trib. Trans.**, 43 (2000), p. 39-44.